ISSN 1070-3632, Russian Journal of General Chemistry, 2015, Vol. 85, No. 10, pp. 2386–2394. © Pleiades Publishing, Ltd., 2015.

Organotin(IV) Complexes with 5-Aminoisophthalic Acid: Synthesis, Characterization, Theoretical Study, and Biological Activities[1]

S. Hussain[a], S. Ali[b], S. Shahzadi[b], S. K. Sharma[c], K. Qanungo[c], M. Shahid[d], A. Jabbar[a], and I. H. Bukhari[a]

[a] *Department of Chemistry, GC University, Faisalabad, Pakistan*

[b] *Department of Chemistry, Quaid-i-Azam University, Islamabad, 45320 Pakistan*
e-mail: drsa54@hotmail.com; sairashahzadi@hotmail.com

[c] *Department of Applied Science and Humanities, Faculty of Engineering and Technology, Mody Institute of Technology and Science (Deemed University), Lakshmangargh, Sikar, Rajasthan 332311, India*

[d] *Department of Chemistry and Biochemistry, University of Agriculture, Faisalabad, Pakistan*

Received July 31, 2015

Abstract—Organotin(IV) carboxylates with the general formula $[Bu_2(Cl)Sn]_2L$ (**1**), $(Me_3Sn)_2L$ (**2**), and $(Bu_3Sn)_2L$ (**3**) were synthesized by stirring 5-aminoisophthalic acid with KOH in methanol and with following addition of Bu_2SnCl_2/Me_3SnCl/Bu_3SnCl under stirring conditions. The complexes were characterized by the microanalysis, IR, and ^1H NMR spectroscopies, mass spectrometry, and by the DFT and semi-empirical methods. The data on the elemental analysis and mass fragmentation agree well with the chemical composition of the complexes. The IR spectroscopy demonstrated a chelating coordination mode of the carboxylate group. The ^1H NMR spectroscopy confirmed the 5-coordinated geometry of the organotin(IV) derivatives. The DFT and semi-empirical calculation of the complex **2** supported an asymmetric coordination behavior of the carboxylate group. The complexes **2** and **3** exhibited an intercalating binding with salmon sperm DNA. Significant antibacterial/antifungal potential of the complexes was confirmed by the disc diffusion method and evaluation of the minimum inhibitory concentration (MIC). The hemolytic activity of the complexes is higher than that of a free ligand and PBS and sufficiently lower than that of triton X-100.

Keywords: organotin(IV) carboxylates, 5-aminoisophthalic acid, spectroscopy, semi-empirical method, DFT, salmon sperm DNA, antimicrobial activity, hemolytic activity

DOI: 10.1134/S1070363215100266

INTRODUCTION

Organotin(IV) complexes are known for their outstanding structural diversity and applications [1]. The complexes have a fascinating variety of structures differing in the coordination numbers and molecular geometries. The difference in structures is correlated with the nature of tin and ligand bonded R groups [2]. Despite the structural diversity of organotin(IV) carboxylates, the number of coordination geometries about of tin is low [2]. The presence of more than one donating entitity in a ligand may increase the coordination number at the Sn(IV) center and may lead to a variety of coordination geometries, such as dimeric, tetrameric, oligomeric ladder, cyclic, drums, polymeric, and other structures [1, 3–5]. The synthesis, properties, and application of heterobimetallic complexes of tin(IV) have been recently studied [6]. Organotin carboxylates continue to be developed as antineoplastic and antituberculosis agents [7], PVC stabilizers [8], anti-tumour drugs [9], and catalysts [10]. The increasing interest in the chemistry of organotin(IV) compounds has led to the extended studies on their reactions with different biomolecules, including carbohydrates [11], nucleic acid derivatives [12], and amino acids [13]. Organtoin(IV) carboxylates are antifungal and antibacterial agents [14]. Keeping in view the great importance of organotin(IV) chemistry, we report here the synthesis, spectroscopic characterization, and DFT and semi-empirical calculation of organotin(IV) complexes with 5-aminoisophthalic acid.

[1] The text was submitted by the authors in English.

The complexes were screened for their antibacterial/antifungal potential and binding with SS-DNA. Their hemolytic activity was also evaluated.

EXPERIMENTAL

Chemicals and instrumentation. Dibutyltin dichloride, trimethyltin chloride, and tributyltin chloride were purchased from Sigma-Aldrich (USA) and used without further purification and 5-Aminoisophthalic acid (**HLH**) was purchased from Merck (Germany). Solvents (all of AR grade) were methanol (Merck), DMSO (Lab-scan), and petroleum ether (Riedel-de Haen). Methanol was dried before use by standard procedure [15].

The samples were taken in capillary tubes and their melting points were measured by a Stuart SMP3 electrochemical melting point apparatus and no correction was done. Elemental analysis was performed on a CHN-932 elemental analyzer (Leco, USA). IR spectra were recorded in the range 4000–400 cm^{-1} on a Perkin-Elmer-1000 FTIR spectrophotometer. The ^1H NMR spectra were measured at 300 MHz on a Bruker ARC 300 MHz-FT-NMR spectrometer. The EI mass spectra were recorded by a Thermo Fisher Exactive Orbitrap instrument, and the electron spin ionization (ESI) mass spectroscopy was carried out with an LTQ XL^{TM} linear ion trap mass spectro-meter (Thermo Scientific).

The structure of the complexes in gas phase was calculated by the DFT method with the Firefly QC package [16], which is partially based on the GAMESS (US) source code [17], using the hybrid B3LYP exchange-correlation functional [18, 19] and the Hay-Wadt Effective Core Potential [20] (with *d* and *p* polarization functionals). The semi-empirical study was done by the MOPAC 2007 [21] program in gas phase using the PM3 method [22, 23]. The selected parts of the complexes not containing the metal ion were pre-optimized by the molecular mechanics methods. Several cycles of energy minimization were carried out for each molecule. The geometry was optimized using eigen vector following method. The root mean square gradient for molecules was always less than unity. A self consistent field was achieved in each case. The absence of the imaginary frequencies was checked to confirm the global minimum in both methods.

The interaction with salmon sperm DNA (SS-DNA) was determined by the reported procedure [24].

Scheme 1. Numbering of the free ligand (**HLH**) and organic groups attached to Sn.

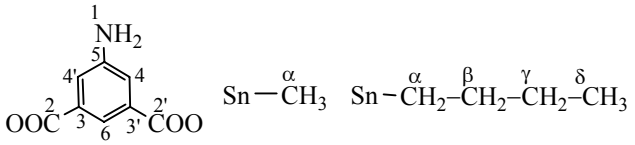

Their antibacterial/antifungal activity was confirmed by the disc diffusion method [25] and from evaluation of the minimum inhibitory concentrations (MIC) [26]. Nutrient agar, nutrient broth, potato dextrose agar, and sabouraud dextrose agar (all from Oxford, U.K.) were used as growth media. The antimicrobial tests were performed in a Sanyo incubator (Germany) and petri plates were sterilized in an Omron autoclave (Japan). The minimum inhibitory concentration was determined in a BioTek Micro Quant apparatus (USA). The in vitro hemolytic bioassay [27] of the complexes is given with respect to triton X-100 and phosphate-buffered saline (PBS) as a standard.

General procedure for synthesis of complexes 1–3. Complexes **1–3** were prepared by slightly modified procedure [14]. **HLH** (1 mmol) and KOH (2 mmol) were placed into a 100-mL round bottom flask, to which 50 mL of ethanol was added, and stirred for 1 h in at room temperature. Then, solid R_2SnCl_2/R_3SnCl (2 mmol) was added in portions and the reaction mixture was continuously stirred for 5 h. The KCl precipitate was filtered off, the solvent was evaporated in a rotary evaporator under reduced pressure, and complexes **1–3** were recrystallized from methanol and petroleum ether (2 : 1) (Schemes 1, 2).

HLH. mp >300°C. IR spectrum, ν, cm^{-1}: 3671 (O–H), 3266 (N–H), 1718 (asym., OCO), 1445 (sym., OCO), ($\Delta\nu$ = 273 cm^{-1}).

Complex 1. Yield: 84%. mp 154–155°C. Calculated, %: C 40.26; H 5.77; N 1.96. $C_{24}H_{41}Cl_2NO_4Sn_2$. Found, %: C 40.22; H 5.80; N 1.94%. IR spectrum, ν, cm^{-1}: 3243 (N–H), 1564 (asym., COO), 1456 (sym., COO), ($\Delta\nu$ = 108 cm^{-1}), 550 (Sn–C), 442 (Sn–O). ^1H NMR spectrum (DMSO-d_6, δ, ppm): 3.42 s (H^1, 2H), 7.37 s ($H^{4,4'}$, 2H), 7.65 s (H^6, H), 1.23–1.35 m (H^α, 8H), 1.60–1.70 m (H^β, 8H), 1.54 t (H^γ, 8H), 0.85 t (H^δ, 12H).

Complex 2. Yield: 66%. mp 220–221°C. Calculated, %: C 33.18; H 4.57; N 2.76. $C_{14}H_{23}NO_4Sn_2$. Found, %: C 33.22; H 4.60; N 2.80. IR spectrum, ν, cm^{-1}: 3257 (N–H), 1560 (asym., COO), 1458 (sym., COO), ($\Delta\nu$ = 102 cm^{-1}), 555 (Sn–C), 441 (Sn–O). ^1H NMR

Scheme 2.

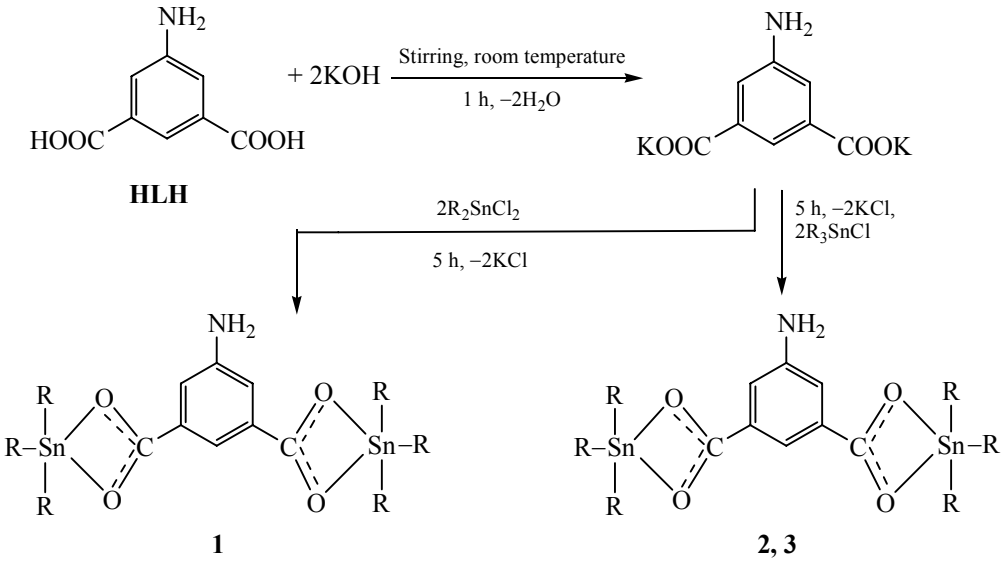

1: R = Bu; **2**: R = Me; **3**: R = Bu.

spectrum (DMSO-d_6, δ, ppm): 3.18 s (H^1, 2H), 6.59 d ($H^{4,4'}$, 2H), 7.32 t (H^6, H), 0.25 s (H^{α}, 18H).

Complex 3. Yield: 95%. mp 170–172°C. Calculated, %: C 50.62; H 7.83; N 1.84. $C_{32}H_{59}NO_4Sn_2$. Found, %: C 50.66; H 7.87; N 1.80. IR spectrum, ν, cm^{-1}: 3236 (N–H), 1584 (asym., COO), 1445 (sym., COO), (Δν = 139 cm^{-1}), 517 (Sn–C), 451 (Sn–O). ^1H NMR spectrum (DMSO-d_6, δ, ppm): 7.38 d ($H^{4,4'}$, 2H), 7.68 t (H^6, H), 1.09 t (H^{α}, 12H), 1.53–1.61 m (H^{β}, 12H), 1.22–1.32 m (H^{γ}, 12H), 0.85 t (H^{δ}, 18H).

Study of DNA interaction. The interaction of the organotin(IV) complexes with SS-DNA was studied by the absorption spectroscopy [24]. To do this, we prepared a solution of SS-DNA in tris-HCl buffer [5 mM tris(hydroxyl methyl)aminomethane and a 50 mM NaCl, pH = 7.2]. The absorbance ratio was 1.9 : 1 at 260 and 280 nm, indicating that DNA is free from protein [28, 29]. The DNA concentration was measured at 260 nm by using the molar absorption coefficient of 6600 M^{-1} cm^{-1} and was found to be 7.45×10^{-5} M [29]. A 2-mM solution of each complex was prepared in a 90% DMSO. For UV-Vis absorption titrations, working solutions (2 mL each) of a test compound and SS-DNA in a 90% DMSO were prepared. The concentration of the complex in these solutions was the same (2 mM), whereas the SS-DNA concentration was different (10, 19, 27, 35, 42, 48, 54, 59, 64, and 69 μM). To eliminate DNA absorbance, we used an equivalent volume of a solution containing SS-DNA and pure solvent as a reference standard. The solutions were incubated at ambient temperature for 30 min. before performing the measurements. Absorption spectra were recorded in a 1-cm cuvettes of 1 cm path length [24].

The binding constant was calculated by the Benesi–Hildebrand equation [30]:

$$\frac{A_0}{A - A_0} = \frac{\varepsilon_G}{\varepsilon_{H-G} - \varepsilon_0} + \frac{\varepsilon_G}{\varepsilon_{H-G} - \varepsilon_G} \times \frac{1}{K[\mathrm{DNA}]},$$

where K is the binding constant, A_0 and A are the absorbances of the drug and its complex with DNA, respectively, and ε_G and ε_{H-G}, the absorption coefficients of the drug and the drug-DNA complex.

The association constants were obtained from the intercept-to-slope ratios of $A_0/(A - A_0)$ vs. 1/[DNA] plots. The Gibbs free energy (ΔG) of the products was determined from the equation:

$$\Delta G = -RT \ln K,$$

where K is the equilibrium constant, R is universal gas constant (8.314 J K^{-1} mol^{-1}), and T, temperature (298 K).

Biological activity. The bacterial strains were cultured in nutrient agar medium at 37°C for overnight and were maintained in the medium in slants and petri plates. Then 10 μL of a pure bacterial culture was added to a 100 mL of an autoclaved (at 121°C for 15 min) nutrient broth medium (100 mL) which was

then incubated in a shaker (140 rpm) at 37°C for 24 h. The prepared inocula were stored at 4°C. The inocula with 1×10^8 spores/mL were used for further analysis. The fungal strains were cultured in potato dextrose agar medium for overnight at 28°C. The pure cultures were maintained in sabouraud dextrose agar (SDA) in slants and petri plates which were presterilized in hot air oven at 180°C for 3 h. These cultured slants were incubated at 28°C for 3–4 days for the multiplication of fungal strains [24]. Antibacterial and antifungal activities were determined by the disc diffusion method [25].

Small filter paper discs (9 mm size), each soaked with a 100 μL of sample solution (1 mg/mL in DMSO), were placed flat on a growth medium (nutrient agar for bacteria and potato dextrose agar for fungi) containing microbes and the petri plates were incubated at 37°C for 24 h for bacterial growth and for 48 h at 28°C for fungal growth. The inhibition zones were measured by a zone reader. The MIC was evaluated by the procedure [24], which is a slight modification of the procedure [26].

Hemolytic activity. Heparinized human blood was freshly collected from volunteers after consent. The in vitro hemolytic activities of the complexes were then found by a reported procedure [27]. For each assay, 0.1% Triton X-100 was used as positive control (100% lysis) and PBS, as negative control (0% lysis). Absorbance at 576 nm was measured on a microquant. Three independent measurements were performed. Percent hemolysis was found by the following formula [27]:

$$\text{Hemolysis} = \frac{\text{Abs}_{\text{sample}}}{\text{Abs}_{\text{control}}} \times 100\%.$$

RESULTS AND DISCUSSION

IR spectroscopy. The data on the IR spectroscopy of the ligand (**HLH**) and complexes **1–3** are summarized in Experimental. In spectra of complexes **1–3**, the ν_{OH} stretching vibration (3671 cm^{-1}) of the free ligand (**HLH**) is absent, which demonstrates the presence of deprotonated carboxylic acid (COO^-) moieties. The ν_{N-H} stretching vibration of the free ligand changes only slightly upon complexation, which shows that the amino group is not involved into the coordination with metal [14]. The carbonyl stretching frequencies of the ligand (**HLH**) decrease upon complexation, which is due to the metal-carboxylate interaction [31]. A carboxylate binding mode can be predicted from the $\Delta\nu = \nu_{as}(COO) - \nu_s(COO)$ value; the smaller $\Delta\nu$ value, the higher the coordination symmetry of carboxylate groups. The $\Delta\nu$ values within 102–139 cm^{-1} in the complexes **1–3** demonstrate the bidentate coordination of carboxylate group [32]. The bidentate coordination behavior of COO^- moieties is also confirmed by the semi-empirical calculation of the complex **2** [33]. The spectra of complexes contain the ν_{Sn-C} and ν_{Sn-O} vibration bands at 517–555 and 441–451 cm^{-1}, respectively, which also confirms complexation [33].

Table 1. C–Sn–C angles (deg) based on ^{1}H NMR parameters

Comp. no.	$^2J(^{119}Sn, ^1H)$, Hz	Angle $\theta(^2J)$, deg
2	71.2	118.7

^{1}H NMR spectroscopy. The ^{1}H NMR spectra were recorded in DMSO-d_6; the data are summarized in Experimental section. The chemical shifts at 3.42 and 3.18 ppm (singlet) in the spectra of complexes **1** and **2**, respectively, were assigned to imino protons. The absence of the –NH signal in complex **3** may be due to the exchange of its proton with deuterium from of DMSO-d_6. The complex **2** showed a singlet at 0.25 ppm, which is due to a trimethyltin(IV) moiety. The observed $^2J[^{119}Sn, ^1H]$ values were used to determine the Me-Sn–Me bond angles in a solution state using the Lockhart–Manders equation [34].

$$\theta = 0.0105[^2J]^2 - 0.799[^2J] + 122.4 \text{ (for coordinating solvents).}$$

Table 1 presents the coupling constants (^nJ) obtained from the resolved satellites and the calculated C−Sn−C bond angles (q) in a coordinating solvent. The ^{1}H NMR spectra of complex **2** strongly support its trigonal bipyramidal geometry. The spectra of complexes 1 and 3 have a clearly resolved triplet at 0.85 ppm, which is due to the terminal methyl group, with $^3J(^1H, ^1H) = 7.2$ Hz [14] and a complex pattern of *n*-butyl fragments.

Mass spectrometry. For complexes **1** and **2**, the electron ionization mass spectra (EI-MS) were recorded and for complex **3**, the electrospray ionization (ESI) mass spectra were measured. Data on the mass fragmentation are summarized in Table 2. The fragment ions containing tin(IV) appeared in the spectrum as a series of close isotopic peaks. The relative intensities reported here were qualitatively estimated from the ion current for the ^{120}Sn peak and must be regarded as approximate.

Table 2. Mass spectral data for complexes **1**–**3**

Comp. no.	MS, *m/z*, %
1	$[C_{24}H_{41}Cl_2NO_4Sn_2]^+$ 718 (n.o)[a], $[C_{24}H_{40}Cl_2NO_4Sn_2]^+$ 717 (3), $[C_{24}H_{41}ClNO_4Sn_2]^+$ 683 (14), $[C_{24}H_{40}ClO_4Sn_2]^+$ 668 (14), $[C_{16}H_{23}ClNO_4Sn]^+$ 448 (61), $[C_{15}H_{23}ClNO_2Sn]^+$ 404 (33), $[C_8H_{18}ClSn]^+$ 269 (23), $[SnCl]^+$ 155 (19), $[C_4H_8]^+$ 56 (100)
2	$[C_{14}H_{23}NO_4Sn_2]^+$ 509 (4)[a], $[C_{12}H_{23}NSn]^+$ 421 (10), $[C_{11}H_{14}NO_4Sn]^+$ 344 (2), $[C_{10}H_{11}NO_4Sn]^+$ 329 (1), $[C_9H_8NO_4Sn]^+$ 314 (1), $[C_8H_5NO_4Sn]^+$ 299 (10), $[C_{10}H_{14}NO_2Sn]^+$ 300 (10), $[C_8H_5NO_4]^+$ 179 (51), $[C_3H_9Sn]^+$ 165 (100), $[C_2H_6Sn]^+$ 150 (5), $[CH_3Sn]^+$ 135 (62), $[Sn]^+$ 120 (5)
3	Positive mode: $[C_{32}H_{59}NO_4Sn_2]^+$ 761 (n.o)[a], $[C_{32}H_{60}NO_4Sn_2]^+$ 762 (14), $[C_{32}H_{58}O_4Sn_2]^+$ 746 (19), $[C_{28}H_{50}NO_4Sn_2]^+$ 704 (79), $[C_{28}H_{48}NO_4Sn_2]^+$ 702 (100), $[C_{26}H_{50}NSn_2Bu_5]^+$ 616 (72), $[C_{20}H_{31}NO_4Sn_2]^+$ 589 (36), $[C_{19}H_{31}NO_2Sn_2]^+$ 545 (42); $[C_{18}H_{32}NSn_2]^+$ 502 (6), $[C_{12}H_{13}NO_4Sn_2]^+$ 475 (46), $[C_{20}H_{32}NO_4Sn]^+$ 470 (5), $[C_{20}H_{31}O_3Sn]^+$ 439 (47), $[C_{16}H_{23}NO_4Sn]^+$ 413 (4), $[C_{12}H_{14}NO_4Sn]^+$ 356 (6), $[C_6H_5NSn_2]^+$ 331 (8), $[C_8H_5NO_4Sn]^+$ 299 (3), $[C_{12}H_{27}Sn]^+$ 291 (2), $[C_8H_{18}Sn]^+$ 234 (2), $[C_6H_5NSn]^+$ 211 (100), $[C_8H_5NO_4]^+$ 179 (10), $[C_4H_9Sn]^+$ 177 (1), $[Sn]^+$ 120 (10) Negative mode: $[C_{32}H_{59}NO_4Sn_2]^-$ 761 (n.o)[a], $[C_{32}H_{58}NO_3Sn_2]^-$ 744 (9), $[C_{28}H_{50}O_4Sn_2]^-$ 690 (79), $[C_{26}H_{49}NSn_2]^-$ 615 (20), $[C_{19}H_{31}NO_2Sn_2]^-$ 545 (78); $[C_{20}H_{30}NO_3Sn]^-$ 452 (18), $[C_{14}H_{22}NSn_2]^-$ 444 (1), $[C_8H_4NO_4Sn_2]^-$ 416 (4), $[C_8H_4O_4Sn_2]^-$ 404 (8), $[C_{12}H_{15}NO_4Sn]^-$ 357 (1), $[C_6H_6NSn_2]^-$ 332 (3), $[C_{14}H_{22}NSn]^-$ 324 (3). $[C_8H_6NO_4]^-$ 180 (100)

[a] Molecular ion peak $[M]^+$; (n.o) is not observed.

The EI-MS of complex **1** displays M-1 peak at *m/z* = 717 (3%), which is due to loss of a hydrogen radical and M-37 peak at *m/z* = 683 (14%), which corresponds to elimination of chloride radical from the parent species. The signal at *m/z* = 717 (23%) demonstrats the presence of a chlorodibutyltin(IV) fragment. The complex **1** may also decompose into $[C_{16}H_{23}ClNO_4Sn]^+$ *m/z* = 448 (61%), whose decarboxylation leads yields $[C_{15}H_{23}ClNO_2Sn]^+$ *m/z* = 404 (33%). The EI-MS pattern of complex **2** and ESI (positive mode) of complex **3**, which is isostructural to complex **2**, have many common features. Each of these complexes may produce a trialkyltin cation $(R_3Sn)^+$ and $R_3SnOOCLCOO$ (where R = Me, *n*-Bu) species, which further decompose graded onto Sn and SnOOCLCOO fragments, respectively. A low intensity molecular ion peak $[M]^+$ at *m/z* = 509 (4%) appeared only in complex **2**. A complete decarboxylation of complex **2** yields a M-88 signal for $[C_{12}H_{23}NSn]^+$ ion (*m/z* = 421 (10%)). The signal at *m/z* = 179 corresponding to the chemical composition of $[C_8H_5NO_4]^+$ was assigned to deprotonated carboxylate ligand; it appeared after expulsion of both trimethyl- or tributyltin(IV) moieties from the complex **2** or 3. The mass spectrum of complex **3** has peak at *m/z* = 762 (14%) for $[M + 1]^+$ ion. The complex **3** may lose NH and OH radicals in the positive and negative modes, respectively, to form $[C_{32}H_{58}O_4Sn_2]^+$ at *m/z* = 746 (19%) or $[C_{32}H_{58}NO_3Sn_2]^-$ at *m/z* = 744 (9%).

Study of DNA interaction. DNA has generally been accepted as the target for most of the anticancer agents. For the newly synthesized complexes, DNA binding parameters were evaluated by the absorption spectroscopy. The complex **1** did not exhibit any sort of interaction with DNA. The DNA binding activities of the complexes **2** and **3** can be attributed to the presence of trialkytin(IV) moieties, as well as the phenyl group; the presence of a phenyl group facilitates the interaction of the drug with a double stranded DNA [35]. The absorption spectra of complexes **2** and **3** have a single band in at 337.0 and 348.0 nm, respectively. The UV spectra (Figs. 1, 2) show a significant hypochromic effect, which is mainly due to intercalation binding. The spectrum was maintained constant during 24 h, which confirmed stability of the drug-DNA complex.

The determined values of the binding constant for complexes **2** and **3** are 8.5×10^3 M^{-1} and 5.5×10^2 M^{-1}, respectively. Thus, the SS-DNA binding of complex **2** is stronger than of complex **3**. This shows that the small size of tin-bound methyl groups facilitates binding. The determined values of the Gibbs free energy are –22.4 and –15.6 kJ/mol for complexes **2**

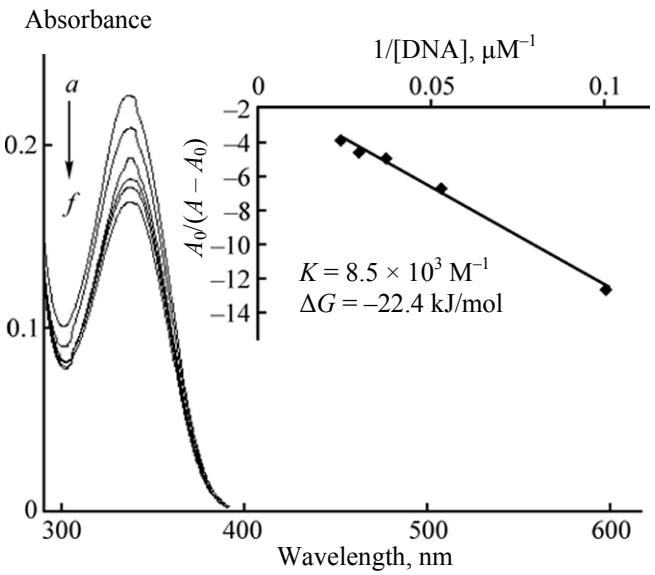

Fig. 1. Absorption spectra of the complex **2** (2 mM) at various concentrations of DNA. DNA concentration, μM: (*a*) 0, (*b*) 10, (*c*) 19, (*d*) 27, (*e*) 35, and (*f*) 42. Increasing DNA concentration is indicated by arrow.

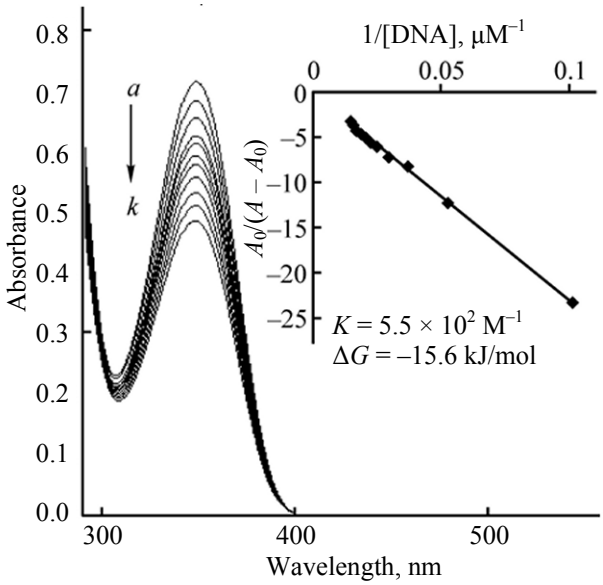

Fig. 2. Absorption spectra of the complex **3** (2 mM) at varied concentrations of DNA. DNA concentration (μM): (*a*) 0, (*b*) 10, (*c*) 19, (*d*) 27, (*e*) 35, (*f*) 42, (*g*) 48, (*h*) 54, (*i*) 59, (*j*) 64, and (*k*) 69. Increasing DNA concentration is indicated by arrow.

and **3**, respectively. The negative ΔG values show that the interaction of the compounds with DNA is a spontaneous process.

Antimicrobial activity. The ligand and the complexes were screened by the disc diffusion method [25] to check their in vitro response against various strains of bacteria and fungi and measure the minimum inhibitory concentration (MIC) [26]. The wells exhibiting MICs were observed visually, while the inhibition zones of the discs were measured by a zone reader. The data are collected in Tables 3, 4.

It was found that the free ligand (**HLH**) is biologically inactive against all tested bacterial and fungal strains [35]. The coordination of ligands with the organotin(IV) moieties induced appreciable antimicrobial activities in the complexes [14]. The increased activity of the complexes **1–3** may be due to the coordination and polarity of the tin(IV) atom with the oxygen atoms of the ligand [36]. In many cases, the antibacterial/antifungal potential of the complexes is very close to that of standard drugs (streptomycin and fluconazole) and in some cases, even exceeds it. This higher activity of the complexes may be due to the multinuclear coordination. However, the antimicrobial potential varies, depending on the coordinated organotin(IV) moieties. A close relationship was observed between the structure and antimicrobial activities of the synthesized complexes; the activities varied, according to the substitution pattern at tin. Among all the investigated complexes **1–3**, complex **1** is most potent antimicrobial drug against the three bacterial (*E. coli, S. aureus* and *P. multocida*) and three fungal (*A. alternate, G. lucidum and A. niger*) strains. The highest antimicrobial activities against *B. subtilis*, *T. harzianum,* and *P. notatum* are exhibited by the complexes **2** and **3**. The complex **2** shows the exceptionally higher antifugal action against *T. harzianum*, with the zone of fungal inhibition 48 mm; this high activity may result from the presence of methyl groups, which enhance the lipophilic character of the ligand.

The results obtained from the determination of minimum inhibitory concentration show that the complexes have generally lower MIC values against the fungi as compared to the bacteria. Complex 3 is active against *A. alternate, G. lucidum, P. notatum, T. harzianum,* and *A. niger* even at the very lowest concentration (μg/mL): 3.3, 1.6, >0.4, >0.4, and 3.3, respectively.

Hemolytic activity. The in vitro hemolytic bioassay of the synthesized complexes were carried out with human red blood cells and the average lysis was reported with respect to the triton X-100 as positive control (100% lysis) and PBS as negative

Table 3. Data on the **a**ntibacterial and antifungal activities

Comp. no.	Bacterial inhibition zone, mm				Fungal inhibition zone, mm				
	E. coli	*B. subtilis*	*S. aureus*	*P. multocida*	*A. alternata*	*G. lucidum*	*P. notatum*	*T. harzianum*	*A. niger*
HLH	–	–	–	-	14^{c}±0.14	$20^{b,c}$±0.09	-	19^{c}±0.12	15^{c}±0.10
1	31^{a}±0.11	$25^{b,c}$±0.29	31^{a}±0.16	30^{a}±0.14	$32^{a,b}$±0.22	$36^{a,b}$±0.16	$27^{b,c}$±0.18	$29^{b,c}$±0.13	$35^{a,b}$±0.23
2	$28^{a,b}$±0.19	$30^{a,b}$±0.25	$26^{b,c}$±0.31	15^{c}±0.22	$22^{b,c}$±0.21	$32^{a,b}$±0.29	20^{c}±0.19	48^{a}±0.28	$28^{a,b}$±0.23
3	15^{c}±0.14	20^{c}±0.14	$30^{a,b}$±0.19	$20^{b,c}$±0.16	$31^{a,b}$±0.12	$36^{a,b}$±0.18	$36^{a,b}$±0.27	$23^{b,c}$±0.13	$29^{a,b}$±0.23
Standard drug	$30^{a,b}$±0.17	$31^{a,b}$±0.28	31^{a}±0.31	$29^{a,b}$±0.28	38^{a}±0.29	41^{a}±0.21	45^{a}±0.31	–	37^{a}±0.23

Concentration is 1mg/mL in DMSO; The table values are the mean ± standard deviation of three independent measurements at $p < 0.1$. Activity: ^{a}(0) absent, ^{a,b}(5–10) present, ^{b,c}(11–25) moderate, and ^{c}(26–40) strong; standard antibacterial and antifungal drugs are streptomycin and fluconazole, respectively.

Table 4. Data on the antibacterial and antifungal activities[a] (minimum inhibitory concentration)

Comp. no.	MIC-bacterial, μg/mL				MIC-fungal, μg/mL				
	E. coli	*B. subtilis*	*S. aureus*	*P. multocida*	*A. alternata*	*G. lucidum*	*P. notatum*	*T. harzianum*	*A. niger*
HLH	-	-	-	-	-	-	-	52	-
1	312	312	156	312	26	26	13	52	-
2	624	624	312	312	52	26	6.5	3.3	13
3	312	39	19.5	39	3.3	1.6	>0.4	>0.4	3.3
Standard drug	1.2	2.4	78	39	26	26	>0.4	-	416

[a] Standard antibacterial and antifungal drugs are streptomycin and fluconazole, respectively.

control (0% lysis). The results obtained are summarized in Table 5.

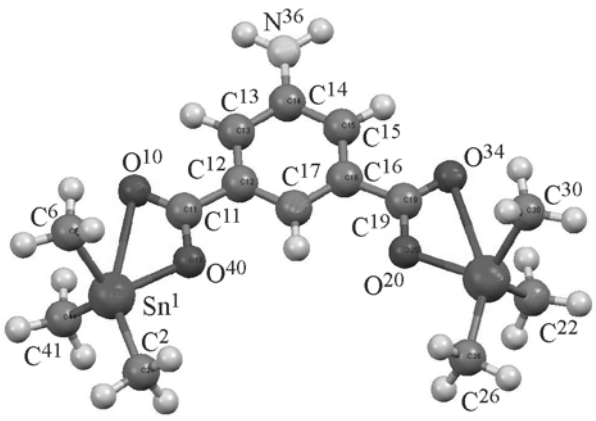

Fig. 3. The computed structure of complex **2**.

The lowest hemolytic activity (14.72%) has free ligand **HLH** and the highest activity (33.06%), complex **2**; the hemolytic activity of other compounds lies within the above values. The hemolytic activity of complexes **1–3** is always higher as compared to free ligand and PBS, whereas sufficiently lower as compared to triton X-100.

DFT and semi-empirical calculation. The computed structure of the complex **2** is symmetrical (see Fig. 3). The bond angles and bond lengths are typical of organotin compounds [2]. The DFT method gives 6.2° for plane between two tin carboxylate groups (Sn–O–C–O) and the semi-empirical PM3 method, 2.90°. The carboxylate oxygen is bound to tin with a longer Sn–O bond, while the carboxylate oxygen with long C–O bond, with a shorter Sn–O bond. This kind of asymmetric coordination is documented in the X-ray crystal structures of organotin carboxylates [2]. The selected bond angles and bond lengths are given in Tables 6 and 7, respectively.

Table 5. Hemolytic activity of free ligand (**HLH**) and complexes

Comp. no.	**HLH**	**1**	**2**	**3**	DMSO	Triton-X 100	PBS
Hemolysis, %	14.72±0.05	23.31±0.02	33.06±0.04	32.52±0.05	9.71±0.05	99.53±0.00	0.00±0.00

Table 6. Selected bond angles (deg) of complex **2**

Bond	O^{20}–Sn^{21}–O^{34}	O^{10}–Sn^{1}–O^{40}	O^{20}–C^{19}–O^{34}	O^{10}–C^{11}–O^{40}
Semi-empirical (PM3)	50.3	50.3	110.4	110.5
DFT (B3LYP/HW)	51.3	51.3	120.5	120.5
Bond	C^{16}–C^{19}–O^{20}	C^{12}–C^{11}–O^{10}	C^{16}–C^{19}–O^{24}	C^{12}–C^{11}–O^{40}
Semi-empirical (PM3)	121.6	121.6	127.9	127.9
DFT (B3LYP/HW)	115.5	115.5	123.9	124.0
Bond	C^{30}–Sn^{21}–C^{22}	C^{22}–Sn^{21}–C^{26}	C^{26}–Sn^{21}–C^{30}	C^{41}–Sn^{1}–C^{6}
Semi-empirical (PM3)	114.2	109.8	109.8	114.2
DFT (B3LYP/HW)	115.0	112.0	112.1	115.0
Bond	C^{6}–Sn^{1}–C^{2}	C^{41}–Sn^{1}–C^{2}	–	–
Semi-empirical (PM3)	109.8	109.8	–	–
DFT (B3LYP/HW)	112.1	112.0	–	–

Table 7. Selected bond lengths (Å) of the complex **2**

Bond	Sn^{21}–O^{34}	Sn^{1}–O^{40}	Sn^{21}–O^{20}	Sn^{1}–O^{10}	C^{19}–O^{20}
Semi-empirical (PM3)	2.71	2.71	2.03	2.03	1.32
DFT (B3LYP/HW)	2.89	2.89	2.01	2.01	1.36
Bond	C^{11}–O^{10}	C^{19}–O^{34}	C^{11}–O^{40}	Sn^{21}–C^{26}	Sn^{21}–C^{30}
Semi-empirical (PM3)	1.32	1.24	1.24	2.11	2.10
DFT (B3LYP/HW)	1.36	1.25	1.25	2.16	2.16
Bond	Sn^{21}–C^{22}	Sn^{1}–C^{41}	Sn^{1}–C^{6}	Sn^{1}–C^{2}	–
Semi-empirical (PM3)	2.10	2.10	2.10	2.11	–
DFT (B3LYP/HW)	2.16	2.16	2.16	2.16	–

CONCLUSIONS

The FTIR spectra of the complexes demonstrate the bidentate binding of carboxylate groups. This coordination mode is also confirmed by the DFT and semi-empirical calculations. The complexes retain their solid state 5-coordinate geometry around the Sn(IV) ion even in the solution. Data on the elemental analysis and results of the EI-MS and ESI spectra are in good agreement with the molecular composition of the complexes. The complexes **2** and **3** exhibit binding with salmon sperm DNA, which is accompanied by a significant hypochromic effect and suggests the intercalating mode of binding. All complexes **1–3** are potent antibacterial/antifungal agents, exhibiting, however, toxic hemolytic effects.

ACKNOWLEDGMENTS

The study was financially supported by the Higher Education Commission, Islamabad, Pakistan (Pin Code 074-3160-Ps4-362).

REFERENCES

1. Abbas, S.M., Ali, S., Hussain, S.T., and Shahzadi, S., *J. Coord. Chem.,* 2013, vol. 66, p. 2217.
2. Shahzadi, S. and Ali, S., *J. Iran. Chem. Soc.,* 2008, vol. 5, p. 16.
3. Tiekink, E.R.T., *Appl. Organomet. Chem.,* 1991, vol. 5, p. 1.
4. Hussain, S., Ali, S., Shahzadi, S., and Rizzoli, C., *Phosphorus, Sulfur, Silicon Relat. Elem.,* 2013, vol. 188, p. 812.
5. Matela, G. and Amman, R., *Cent. Eur. J. Chem.,* 2012, vol. 10, p. 1.
6. Hussain, S., Ali, S., Shahzadi, S., and Shahid. M., *Cogent Chem.,* 2015, vol. 1, http://dx.doi.org/10.1080/23312009.2015.1029038.
7. Zhang, X., Yan, H., Song, Q., Liu, X., and Tang, L., *Polyhedron,* 2007, vol. 26, p. 3743.
8. Arks, E., and Balko, D., *Polym. Degrad. Stab.,* 2005, vol. 88, p. 46.
9. Seinen, W. and Willems, M.I., *Toxicol. Appl. Pharmacol.,* 1976, vol. 35, p. 63.
10. Tariq, M., Ali, S., Muhammad, N., Shah, N.A., Sirajuddin, M., Tahir, M.N., Khalid, N., and Khan, M.R., *J. Coord. Chem.,* 2014, vol. 67, p. 323.
11. Barbieri, R., Silvertri, A., and Piro, V., *J. Chem. Soc. Dalton Trans.,* 1990, vol. 12, p. 3605.
12. Buzas, N.N., Gajda, T., Kuzmann, E., Vertes, A., and Burger, K., *Main Group Met. Chem.,* 1995, vol. 11, p. 641.
13. Preut, H., Vornefeld, M., and Huber, F., *Acta Crystallogr.*, 1991, vol. C47, p. 264.
14. Hussain, S., Ali, S., Shahzadi, S., Sharma, S.K., Qanungo, K., and Shahid, M., *Bioinorg. Chem. Appl.,* 2014, vol. 2014, p. 1.
15. Armarego, W.L.F. and Chai. C.L.L., *Purification of Laboratory Chemicals,* London: Butterworth Heinemann, 2003.
16. Granovsky, A.A., *Firefly version 7.1.G*, www.http://classic.chem.msu.su/gran/firefly/index.html.
17. Schmidt, M.W., Baldridge, K.K., Boatz, J.A., Elbert, S.T., Gordon, M.S., Jensen, J.H., Koseki, S., Matsunaga, N., Nguyen, K.A., Su, S., Windus, T.L., Dupuis, M., and Montgomery, J.A., *J. Comput. Chem.,* 1993, vol. 14, p. 1347.
18. Becke, A.D., *J. Chem. Phys.,* 1993, vol. 98, p. 5648.
19. Stephens, P.J., Devlin, F.J., Chabalowski, C.F., and Frisch, M.J., *J. Phys. Chem.,* 1994, vol. 98, p. 11623.
20. Hay, P.J. and Wadt, W.R., *J. Chem. Phys.,* 1985, vol. 82, p. 270.
21. Stewart, J.J.P., *MOPAC2007,* Stewart Computational, Chemistry, Version: 7.334W.
22. Stewart, J.J.P., *J. Comput. Chem.,* 1991, vol. 12, p. 320.
23. Stewart, J.J.P., *J. Comput. Chem.,* 1989, vol. 10, p. 209.
24. Hussain, S., Ali, S., Shahzadi, S., Tahir, M.N., and Shahid, M., *J. Coord. Chem.,* 2015, vol. 68, p. 2369.
25. CLSI (The Clinical Laboratory Standards Institute), *J. Clin. Microbiol.,* 2007, vol. 45, p. 2758.
26. Sarker, S.D., Nahar, L., and Kumarasamy, Y., *Methods,* 2007, vol. 42, p. 321.
27. Sharma, P. and Sharma, J.D., *J. Ethnophamacol.,* 2001, vol. 74, p. 239.
28. Zhang, Y., Wang, X., and Ding, L., *Nucleos. Nucleot. Nucl.,* 2011, vol. 30, p. 49.
29. Sastri, C.V., Eswaramoorthy, D., Giribabu, L., and Maiya, B.G., *J. Inorg. Biochem.,* 2003, vol. 94, p. 138.
30. Ahmad, M.S., Hussain, M., Hanif, M., Ali, S., and Mirza, B., *Molecules,* 2007, vol. 12, p. 2348.
31. Baul, T.S.B., Dhar, S., Pyke, S.M., Tiekink, E.R.T., Rivarola, E., Butcher, R., and Smith, F.E., *J. Organomet. Chem.,* 2001, vol. 633, p. 7.
32. Deacon, G.B. and Phillips. R., *J. Coord. Chem. Rev.,* 1980, vol. 33, p. 227.
33. Iqbal, H., Ali, S., Shahzadi, S., Sharma, S.K., Qanungo, K., and Shahid, M., *J. Coord. Chem.,* 2015, vol. 68, p. 2434.
34. Lockhart, T.P., Manders, W.F., and Holts, E.M., *J. Am. Chem. Soc.,* 1986, vol. 108, p. 6611.
35. Javed, F., Ali, S., Shah, M.W., Munawar, K.S., Shahzadi, S., Ullah, H., Fatima, H., Ahmed, M., Sharma, S.K., AND Qanungo, K., *J. Coord. Chem.,* 2014, vol. 67, p. 2795.
36. Singh, N., Gupta, S., and Nath, G., *Appl. Organomet. Chem.,* 2000, vol. 14, p. 484.